COBEM 2021 26th International Congress of Mechanical Engineering
ABCM Associação Brasileira de Engenharia e Ciências Mecânicas
November 22-26, 2021, Virtual Congress, Brazil

COB-2021-0656
Fatigue assessment in Frequency domain of Gaussian stress-time histories with varying irregularity factors

Thiago Nogueira dos Santos
Jorge Alberto Rodriguez Durán
Universidade Federal Fluminense, Av. dos Trabalhadores, 420 - Vila Santa Cecília, Volta Redonda, RJ, Brazil
thiagonds@id.uff.br
jorge.a.r.duran@gmail.com
Juliano Carvalho da Silva Filho
Volkswagen Caminhões e Ônibus, Rua Volkswagen, 100 - Resende, RJ, Brazil
julianocsfilho@gmail.com

Abstract. *This paper is dedicated to the study of fatigue of materials through frequency domain-based methods to estimate the fatigue life for Gaussian stress-time histories. The rainflow cycle counting RFCC method is considered the most suitable procedure for cycle counting of varying amplitudes stress-time histories. For random loadings, however, the fatigue damage based on these histories, even when calculated by the RFCC, is clearly a random variable and numerous records are needed to infer some important characteristics such as the mean damage intensity. The frequency domain methods, on the other hand, exhibit some advantages over the traditional time domain methods and so will be addressed in the present paper. Four simulated stress histories with different irregularity factors* α_2 *were used for comparing the damage intensity predicted by four frequency domain-based methods with that computed using the RFCC approach. The results that were closest, and still conservative, to those of the RFCC, were provided by Dirlik method.*

Keywords: *Fatigue, Rainflow, life estimation, frequency domain*

1. INTRODUCTION

There are several components of machine and structure that do not reach failure due to yield because they do not suffer enough static stress for this. However it can fail when submitted to repeated efforts — many times significantly below the ultimate strength (S_u) or even yield strength (S_y), which cause microscopic physical damage to the material involved — a crack can appear at a critical area. When specimen undergoes cyclic loads, damage can accumulate until it develops a crack or macroscopic damage that can lead material to fracture. This failure process can be called fatigue (Dowling, 2013; Juvinal and Marshek, 2012).

Long time ago man noticed that these repeated loads cause the material's fracture. As this failure occurs at random, there are cases where the cost may involve human lives unexpectedly. The first commercial passenger jet plane (*Comet*) was shattered in 1954 when pressurization and depressurization cycles caused the fatigue failure of the aircraft (Norton, 2006).

The most important problems of fatigue failure were found about 1850, during the development of an European railway. An initial explanation was that the metal crystallized under repeated loading until failure. The first tests were carried out by Wöhler between 1852 and 1869 (Lalanne, 2014).

In 1964, Bendat proposed the first solution for estimating fatigue life of materials in the frequency domain through Power Spectral Density (hereafter PSD). It was shown by Bendat that the peak probability density function (PDF) for a narrow band history comes close to a Rayleigh distribution using equations formulated by Rice to estimate the number of peaks, using spectral moments data calculated through PSD (Bishop and Sherratt, 2000). This model, however, obtains more reliable results for specific cases in which the stress history is considered to be a Narrow Band, generating very conservative results for broadband. Then, searching to correct this problem observed in Rayleigh, some researchers formulated a way to obtain a correction factor, calculated empirically, for the damage obtained through the Bendat solution, e.g. Wirsching and Light (1980) and Benasciutti and Tovo (2004). Subsequently, others researchers performed methods to estimate the cycle counting predicted by Rainflow, e.g. Dirlik (1985) and Zhao and Baker (1992).

The present work is focused on the comparison of the four methods based on the frequency domain mentioned above, related to the method in the time domain Rainflow, applied to the history of stationary Gaussian processes with different irregularity factors (α_2). The frequency domain methods are preferred over the time domain methods mainly for dealing with random process in linear structures using finite element analysis. While in time domain the structural model must be solved for each point of the input history, in the frequency domain the transfer function, i.e. the system response per unit input at a given frequency, is calculated only once. This allows the PSD for stresses and strains at critical locations to be known by just multiplying the PSD input signal by the system transfer function which has obvious computational advantages.

The structure of this paper can be described as follows: first, the fundamental theoretical background is presented in Sec. 2. After that, the paper shows the selected material and the stress-time histories for each irregularity factor studied in the present work in Sec. 3. The Section 4 was elaborated to present the results obtained by the methods studied, i.e. the comparison of the different approaches, in addition on explaining the values obtained and the meanings of the graphs. Finally, the conclusion is given in Sec. 5.

2. THEORETICAL BACKGROUND

This section will focus on explaining the fundamental insight to understand this article, even as fracture and fatigue study and life estimate based on different methods.

2.1 Fatigue of materials

2.1.1 S-N curve

The result of several tests of different stress levels can be plotted to obtain a curve that illustrates the life of the material (N_f in cycles) for each stress suffered (σ_a in MPa), also called the S-N curve. Linear regression of log-linear ($log(N_f)$, σ_a) of this points allows to obtain constants of materials as σ'_f and b. The graph generated from linear regression is called S-N Curve. In these tests, made to generate SN Curve, $\sigma_m = 0$. The equation of S-N Curve is seen below (Dowling, 2013):

$$\sigma_a = \sigma'_f \left(2N_f\right)^b \tag{1}$$

Where σ'_f is Fatigue Strength — the stress level where $N_f = 1/2$ cycles — and b is the curve slope (Larsen and Irvine, 2015). S-N Curve can also be represented by (2):

$$\sigma_a = A \left(N_f\right)^B \tag{2}$$

Where $A = 2^b \sigma'_f$ and $B = b$.

In fatigue analysis through frequency domain method, it is necessary two material constants, SN slope (k) and C. Handling (2), we can obtain (3):

$$\sigma_a^k N_f = C \tag{3}$$

Where $k = -\frac{1}{B}$ and $C = A^k$.

2.1.2 Palmgren-Miner

In case of some material is subjected of S_{ai} MPa in n_i cycles, part of machine will suffer a damage. If this stress is relieved and a new one is applied in material with a certain number of cycles, the material will experience more damage and it is accumulated until the structure reaches the fracture. Consider D_i as each particular damage (Lalanne, 2014; Budynas and Nisbett, 2006):

$$D_i = \frac{n_i}{N_f i} \tag{4}$$

and

$$D_T = \sum_{i=1}^{m} D_i \tag{5}$$

If damage D_T is greater than or equal to 1 ($D_T \geq 1$), material reaches crack nucleation.

2.2 Power spectral density

To obtain the power spectral density (PSD), it is necessary to calculate the autocorrelation function, which represents how a variable can be correlated with itself and it is given by (Dirlik, 1985; Benasciutti and Tovo, 2004; Lalanne, 2003):

$$R_{XX}(\tau) = E[X(t)X(t+\tau)] \tag{6}$$

Where τ is equivalent to a delay of independent variable t of the stationary random process $X(t)$.

Frequency domain of autocorrelation function represents the called Two-Sided Power Spectral Density, which can be obtained as seen in (7):

$$S_{XX}(f) = \int_{-\infty}^{\infty} R_{XX}(\tau)e^{-i2\pi f\tau}d\tau \tag{7}$$

Thereby, it's possible to generate Power Spectral Density only in positive frequencies as seen below:

$$G_{XX}(f) = \begin{cases} 2S_{XX}(f); & 0 < f < \infty \\ S_{XX}(f); & f = 0 \end{cases} \tag{8}$$

Knowing $G_{XX}(f)$, it is possible to calculate some of important statistical features as well as spectral moments, irregularity factor and probability density function, which will be shown in subsection 2.3.

2.3 Statistical properties

After the passage of the signal from the time domain to the frequency domain through Fourier Transform applied to autocorrelation function of stress history given by (7) and (8), it is indispensable to obtain the four main spectral moments, which depend on the results in frequency domain (One-Sided Power Spectral Density). All spectral moments can be estimate, but only m_0, m_1, m_2 and m_4 are required in fatigue analysis. Spectral moments are calculated by (9) (Benasciutti and Tovo, 2004; Mršnik *et al.*, 2013; Cristofori *et al.*, 2011; Benasciutti *et al.*, 2013):

$$m_n = \int_{0}^{\infty} (2\pi f)^n G_{XX}(f)df \tag{9}$$

Where G_{XX} represents One-Sided Spectral Moments [MPa^2/Hz] and f is frequency [Hz]. When spectral moment index is 0, 2 and 4 spectral moment act as variance of signal (σ_X^2), and its derivatives ($\sigma_{\dot{X}}^2$ and $\sigma_{\ddot{X}}^2$), thus Mršnik *et al.* (2013); Tovo (2002):

$$m_0 = \sigma_X^2 \qquad m_2 = \sigma_{\dot{X}}^2 \qquad m_4 = \sigma_{\ddot{X}}^2 \tag{10}$$

Thereat, it's possible to estimate number of positive mean-crossing and number of peaks, as given by (11), respectively Mršnik *et al.* (2013); Benasciutti (2005):

$$\nu_{0^+} = \frac{1}{2\pi}\sqrt{\frac{m_2}{m_0}} \qquad \nu_p = \frac{1}{2\pi}\sqrt{\frac{m_4}{m_2}} \tag{11}$$

Furthermore, we must calculate spectral width through α_n parameter. Its general form is seen in (12) (Larsen and Irvine, 2015; Benasciutti and Tovo, 2004):

$$\alpha_n = \frac{m_n}{\sqrt{m_0 m_{2n}}} \tag{12}$$

which aims to evaluate frequency distribution of PSD — when α_n comes to unity, there is a narrow-band process and, when it comes to 0, we have a wide-band process (Cristofori *et al.*, 2011).

Instead of time to failure criteria, damage intensity will be obtained $\overline{D}$, estimated in damage per second (Benasciutti *et al.*, 2013). Damage intensity can be obtained through (13).

$$\overline{D} = \nu_p C^{-1} \int_{0}^{\infty} s^k p_a(s)ds \tag{13}$$

Where s is amplitude stress to which the material is subjected and $p_a(s)$ is the Probability Density Function (PDF) of amplitude stress.

The PDF of an amplitude stress ($p_a(s)$) of a random process is a measure of how long a signal remains in a specific amplitude. In general, it's possible to obtain a PDF from (14) (Rice, 1944):

$$p_a(s) = \frac{\sqrt{1-\alpha_2^2}}{\sqrt{2\pi m_0}} \cdot e^{-\frac{s^2}{2m_0(1-\alpha_2^2)}} + \frac{\alpha_2 s}{m_0} \cdot e^{\frac{-s^2}{2m_0}} \cdot \frac{1}{2}\left\{erf\left[\frac{\alpha_2 s}{\sqrt{2m_0(1-\alpha_2^2)}}\right] + 1\right\} \tag{14}$$

Where $erf(\cdot)$ is error function, given by (15):

$$erf(x) = \frac{2}{\sqrt{\pi}} \int_0^x e^{-t^2} dt \tag{15}$$

The evaluation of the frequency domain methods in this present paper is performed by a comparison between fatigue life estimated T in seconds, that can be obtained from damage intensity as seen:

$$T = \frac{1}{\overline{D}} \tag{16}$$

Nevertheless, it is necessary to obtain Probability Density Function before calculating the damage, and it will be done by four different methods in frequency domain, as will be seen in subsection 2.4.

2.4 Frequency domain methods

To be possible to evaluate the damage by (13), it is necessary to obtain the PDF, either by a method in time domain — e.g Rainflow — or by a frequency domain method, which will be presented below.

2.4.1 Rayleigh approximation

Considering a Narrow-Band Process, it is evident the proximity of Rainflow Cycles Counting to Rayleigh Distribution. To calculate this distribution, it is required to consider $\alpha_2 = 1$ in (14) (Dirlik, 1985; Zhao and Baker, 1992; Ariduru, 2004). So, with spectral moments and considering irregularity factor as unity, it is possible to generate PDF of Rayleigh as follows:

$$p_a(s) = \frac{s}{m_0} e^{\frac{-s^2}{2m_0}} \tag{17}$$

In general, this method is suitable for specific cases, generating results more conservative for several stress histories. Thinking about correcting errors generated by this method, correction factors were elaborated.

2.4.2 Correction factors

As seen before, Rayleigh approximation generates over-conservative results for various histories, overall wide-band processes. With this in mind, several researchers began to elaborate methods to correct errors caused by Rayleigh approximation. These methods are based on the ratio seen in Eq. (18).

$$\lambda = \frac{\overline{D}_{RFC}}{\overline{D}_{RL}} \tag{18}$$

where $\overline{D}_{RFC}$ is the Rainflow damage intensity approximation, that will be calculated by methods proposed by some authors — in this paper, two different methods will be presented — $\overline{D}_{RL}$ refers to Rayleigh damage approximation and λ is the correction factor.

$$\overline{D}_{RFC} = \lambda \overline{D}_{RL} \tag{19}$$

For the first correction factor, we must notice that Rainflow fatigue damage presents a possible correlation with some bandwidth parameters, e.g. $\alpha_{0.75}$ (Lutes *et al.*, 1984). Benasciutti and Tovo (2004) proposed an empirical method, considering the correction factor as follows in Eq. (20):

$$\lambda_{AL} = \alpha_{0.75}^2 \tag{20}$$

Moreover, Benasciutti and Tovo (2004) proposed a correction factor that can achieve very approximate values. This correction factor can be seen in Eq. (21)

$$\lambda_{TB} = \left[b + (1-b)\,\alpha_2^k\right] \overline{D}_{RL} \tag{21}$$

where b can be calculated as follows in Eq. (22)

$$b(\alpha_1, \alpha_2) = \min\left\{\frac{\alpha_1 - \alpha_2}{1 - \alpha_1}, 1\right\} \tag{22}$$

2.4.3 Dirlik

Dirlik initially tried different combinations of probability distributions to estimate his probability density functions, such as Gaussian, Rayleigh, erf and Gaussian derivative functions. These attempts were tested to replace exponential term, but the density that presents best results was exponential, even generating densities greater than Rayleigh for low ranges. This method is an mixture of an exponential distribution and two Rayleigh distribution, one considering variable Rayleigh parameter and a standard Rayleigh distribution, as seen below (Dirlik, 1985; Mršnik *et al.*, 2013; Benasciutti and Tovo, 2005):

$$p_a(s) = \frac{\frac{D_1}{Q}e^{\frac{-z}{Q}} + \frac{D_2 z}{R^2}e^{-z^2} + D_3 z e^{\frac{-z^2}{2}}}{\sqrt{m_0}} \tag{23}$$

And all parameters can be obtained as follows:

$$z = \frac{s}{\sqrt{m_0}}; \quad X_m = \frac{m_1}{m_0}\sqrt{\frac{m_2}{m_4}}; \quad D_1 = 2\left(\frac{X_m - \alpha_2^2}{1+\alpha_2^2}\right); \quad R = \frac{\alpha_2 - X_m - D_1^2}{1 - \alpha_2 - D_1 + D_1^2} \tag{24}$$

$$D_2 = \frac{1 - \alpha_2 - D_1 + D_1^2}{1-R}; \quad Q = \frac{5(\alpha_2 - D_1 - D_2 \cdot R)}{4 \cdot D_1}; \quad D_3 = 1 - D_1 - D_2 \tag{25}$$

where z is the normalized stress, X_m is the mean frequency and D_1, D_2, D_3, R and Q are Dirlik Distributions parameters.

2.4.4 Zhao-Baker

Weibull Distribution are often used in several areas of engineering, being a fundamental tool for reliability engineering. This distribution can be seen below (Weibull, 1951):

$$p(z) = \frac{\gamma}{\rho}\left(\frac{z}{\rho}\right)^{\gamma-1} e^{-\left(\frac{z}{\rho}\right)^{\gamma}} \tag{26}$$

Where γ and ρ are Weibull parameters.

However, it is remarkable that a single Weibull distribution is not adequate to model PDF for irregularity factors typical of a Narrow Band. For these cases, a Rayleigh Distribution obtain more reliable results (Zhao and Baker, 1992; Wirsching and Shehata, 1977). The proposal amplitude PDF is described as follows:

$$p_a(s) = \omega\alpha\beta z^{\beta-1}e^{-\alpha z^{\beta}} + (1-\omega)ze^{-\frac{z^2}{2}} \tag{27}$$

where ω is the weighting factor and α and β are Weibull parameters, defined as seen in (28) and (29), respectively:

$$\omega = \frac{1-\alpha_2}{1 - \sqrt{\frac{2}{\pi}}\Gamma\left(1+\frac{1}{\beta}\right)\alpha^{-1/\beta}} \tag{28}$$

$$\alpha = 8 - 7\alpha_2 \qquad \beta = \begin{cases} 1.1; & \alpha_2 < 0.9 \\ 1.1 + 9(\alpha_2 - 0.9); & \alpha_2 \geq 0.9 \end{cases} \tag{29}$$

3. MATERIALS AND METHODS

This section aims to present the selected material, show which stress histories were used for each irregularity factor and perform a comparison between the statistical variables obtained both from the PSD and directly from the stress-time history. The AISI 1020 Hot-Rolled steel was chosen to do the fatigue analysis in this paper and this material has S–N curve slope k = 6.41 and fatigue constant C = 3.41e+19 MPa^k (eFatigue, 2021). In this work, different stress histories was created from the same Random Process, see Fig. 1(a). With this random history created, a normal probability plot – a Graphical Technique that can identify if a random data aproximate to a normal distribution – was built to verify if we were dealing with a Gaussian Process. The straight line (orange line, see Fig. 1(b)) represents the expected values for Gaussian Distribution while the blue data shows the values of the analised sample. If the random process is Gaussian, its derivatives are also Gaussian. The Random Process and the Normal Distribution Plot can be seen in Fig. 1.

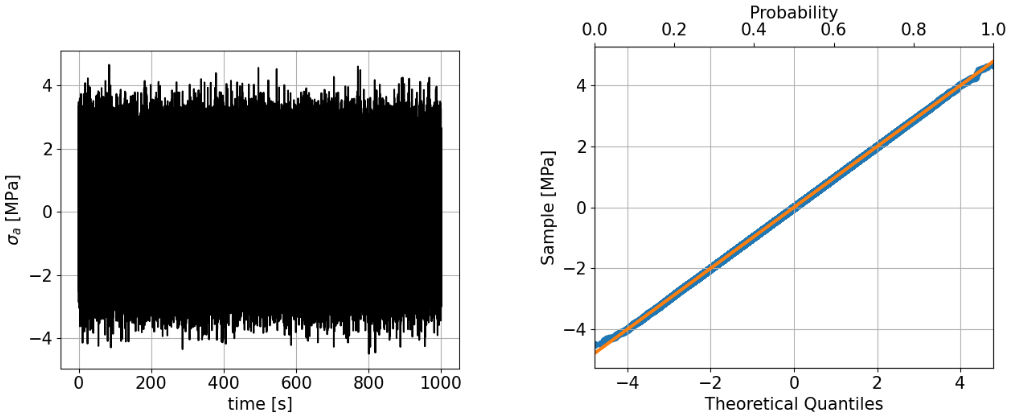

(a) Random Process (b) Normal Distribution Plot

Figure 1. Random Process before applied some steps to generate fatigue histories with varying irregularity factors and normal distribution plot

3.1 Wide band fatigue history

To generate a Wide Band History, a Lowpass filter was applied in random process (Fig. 1(a)) after selecting 200 MPa as its amplitude stress. The cut-off frequency and filter order were selected to generate histories with irregularity factors of 0.30 and 0.58. Both have 30 Hz as cut-off frequency, while the history with $\alpha_2 = 0.30$ has 1 as filter order and history with $\alpha_2 = 0.58$ has 2 as filter order.

3.2 Narrow band fatigue history

Various processes that cause fatigue can be represented by a simple periodic function or by overlapping periodic functions with random amplitudes and frequencies. Such process generates narrow band histories in an explicit way, however, for the present work, histories were built to represent a narrow band applying a Bandpass filter in the same random history that was used for obtained wide band histories.

To generate a Narrow-Band Process, cutoff frequencies were chosen based in sample frequency (threshold must be less than 500 Hz). Initially, a stress history with $\alpha_2 = 0.78$ was obtained selecting 30 and 350 Hz as cut-off frequencies and multiplying the random process by 40 MPa. Finally, a 0.94 irregularity factor was obtained selecting 50 and 120 Hz as cut-off frequencies and the multiplier is 100 MPa.

After the generation of history in time domain, it was necessary to obtain the One-Sided PSD. With the Power Spectral Density obtained for each history under analysis, it was possible to achieve the main spectral moments with the aid of the Eq. 9, fundamentals parameters in Fatigue Analysis through frequency domain methods. Thus, it is possible to calculate the already mentioned irregularity factor to define the bandwidth of each history, the Probability Density Functions and calculate the fatigue damage. Furthermore, the results were compared with the ones obtained by the Rainflow method.

Similar results were noticed when comparing standard deviation of the time-domain history and the square root of the first moment ($\sqrt{m_0}$) of all histories and the same behaviour occurs when comparing the standard deviation of the derivative of the time domain history and the $\sqrt{m_2}$ in addition to the proximity of the number of peaks and the mean upcrossing counted in time domain and the expected values computing by Eq. (11) (ν_p and ν_{0+}). These comparisons is shown in Tab. 1. The time-domain column represents the value of property obtained with the time-domain history and Frequency-domain column shows the values obtained with spectral moments. The values in time domain of property counted (mean upcrossing and peaks frequency) and computed (σ_X and $\sigma_{\dot{X}}$) in addition to properties calculated in frequency domain were obtained through a Python Program developped for this research.

4. RESULTS AND DISCUSSION

4.1 Histograms for the amplitude stress in time and frequency domains

In this section, a comparison was done between all methods analised in present paper. Considering the PDFs of amplitudes obtained by the methods in the frequency domain, it is possible to make a conversion from PDF to number of cycles, allowing then the comparison between the graphs obtained by each method. This conversion was done as follows:

$$n(s_i) = p_a(s_i) \cdot ds \cdot \nu_p \cdot T \tag{30}$$

Table 1. Statistical properties in the time and frequency domains.

Irregularity Factor	**Property**	**Frequency-domain**	**Time-domain**
0.30	σ_X	43.3	43.2
	$\sigma_{\dot{X}}$	7251.3	7168.8
	ν_0	27	25
	ν_p	88	90
0.58	σ_X	44.7	44.6
	$\sigma_{\dot{X}}$	4842.7	4832.1
	ν_0	17	17
	ν_p	30	24
0.78	σ_X	30.3	30.3
	$\sigma_{\dot{X}}$	35950.6	32608.3
	ν_0	189	181
	ν_p	243	230
0.94	σ_X	32.0	32.1
	$\sigma_{\dot{X}}$	16680.5	16521.7
	ν_0	83	84
	ν_p	88	90

The blue dashed, orange dashdot, green solid and red dashed line represent PDF of $\alpha_{0.75}$, Tovo-Benasciutti, Dirlik and Zhao-Baker methods, respectively, as can be seen in Fig. 2.

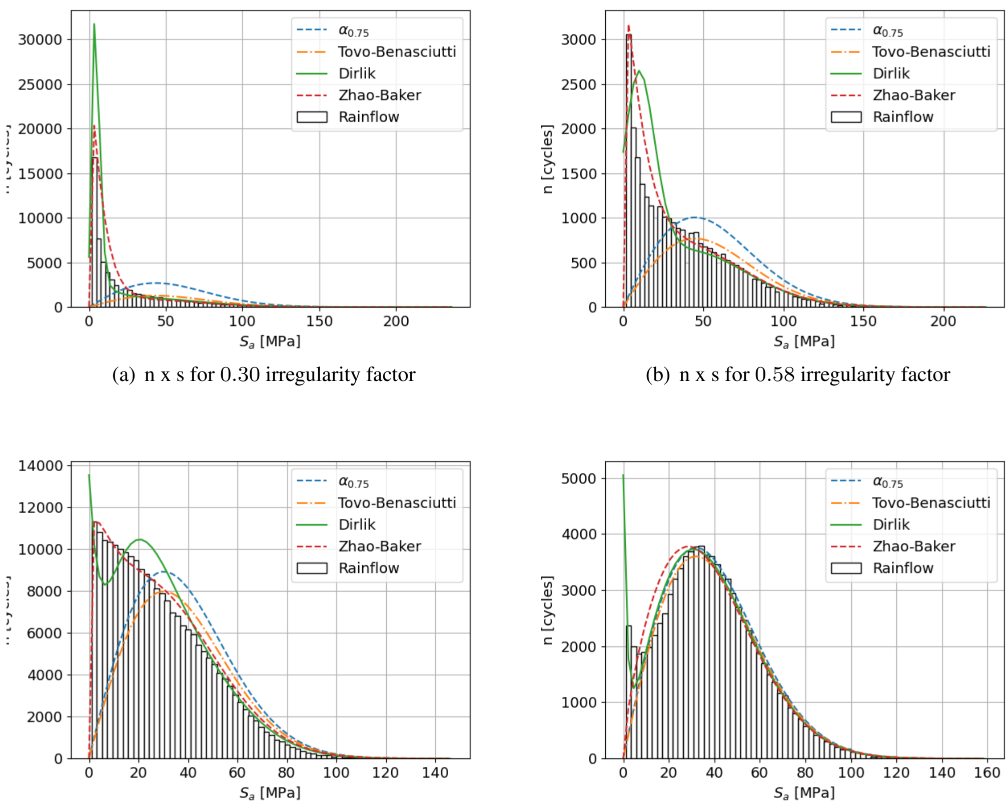

(a) n x s for 0.30 irregularity factor

(b) n x s for 0.58 irregularity factor

(c) n x s for 0.78 irregularity factor

(d) n x s for 0.94 irregularity factor

Figure 2. Comparison of plots n x s for different irregularity factors.

Analysing Fig. 2, when looked at the cycle counting of history with α_2 0.94 (Fig. 2(d)), it is possible to notice a good approximation of cycle counting of the four methods, which allowed to achieve favourable results. For the PDFs of history with α_2 0.78 (Fig. 2(c)), the cycle counting made by the frequency domain-based methods is closer to the histogram in medium to high stresses, but not to lower stresses, however these lower stresses do not so much influence on the calculated damage, what allows the fatigue life prediction for the selected material to remain quite approximate when calculated by these methods. For cycle counting seen in Fig. 2(b) ($\alpha_2 = 0.58$), lower stresses do not present an approximate cycle counting when comparing frequency domain methods and Rainflow too, but medium and high do, similar to what was observed in Fig. 2(c). Finally, we can notice that the cycle counting by frequency domain-based methods generated by Gaussian stress-time history with irregularity factor equal to 0.30 strongly resemble to Rainflow Histogram, especially for medium and high amplitudes, see Fig. 2(a).

Considering that the four stress histories seen in Sec. 3 is applied on a steel AISI 1020 Hot-Rolled bar, the Tab. 2 shows values of Damage intensity, N_f – which represent the number of repetitions of the histories described in Sec. 3 until failure – and Life estimate (in hours) for all four methods in frequency-domain and for Rainflow method.

Table 2. Comparison of Damage and Life of a steel 1020 Hot-Rolled when applied different stress history with varied α_2.

Irregularity factor	Method	Damage intensity [D/s]	N_f [cycles]	Life estimate [hours]
0.30	Rainflow	1.07057e-06	934	259
	$\alpha_{0.75}$	3.68149e-06	271	75
	Tovo-Benasciutti	1.74722e-06	572	158
	Dirlik	1.18481e-06	844	234
	Zhao-Baker	1.01218e-06	987	274
0.58	Rainflow	9.24397e-07	1081	300
	$\alpha_{0.75}$	1.80664e-06	553	153
	Tovo-Benasciutti	1.38054e-06	724	201
	Dirlik	1.07267e-06	932	258
	Zhao-Baker	1.10079e-06	908	252
0.78	Rainflow	7.51883e-07	1329	369
	$\alpha_{0.75}$	1.39057e-06	719	199
	Tovo-Benasciutti	1.24320e-06	804	223
	Dirlik	9.98627e-07	1001	278
	Zhao-Baker	1.08507e-06	921	256
0.94	Rainflow	7.17933e-07	1392	386
	$\alpha_{0.75}$	8.13035e-07	1229	341
	Tovo-Benasciutti	7.79729e-07	1282	356
	Dirlik	7.41172e-07	1349	374
	Zhao-Baker	7.29041e-07	1371	381

When running the program that generate the results seen in Tab. 2, it was possible to check the processing time for each method used in the work. The Rainflow took about 3 seconds to complete the calculations of Damage and Life, while the $\alpha_{0.75}$ and Tovo-Benasciutti methods took 0.35 seconds and the Dirlik and Zhao-Baker methods took 0.19 seconds. It is logical that the Dirlik and Zhao-Baker methods take less time than $\alpha_{0.75}$ and Tovo-Benasciutti to obtain the results, since the $\alpha_{0.75}$ and Tovo-Benasciutti need to obtain the Rayleigh PDF and after that it is calculated the correction factor, what makes the methods slower, while Dirlik and Zhao-Baker only need the calculation of PDFs to reach their results.

Furthermore, it is possible to verify the proximity of results through a cumulative spectrum plot, which gives the number of cycles with stress amplitudes above or at the same level than S_a. This is an alternative way for presenting the results of the various counting procedures. Analysing the graphs, the cumulative cycles of all methods are close to the Rainflow spectrum for all irregularity factor, but it is closer for 0.78 and 0.99. As the α_2 decreases, the loading spectra of frequency domain-based methods move away from the Rainflow spectrum. This graph can be seen in Fig. 3.

Analysing the 1020 hot-rolled steel, after calculating error related to number of cycles to failure when comparing each frequency domain-based method with Rainflow Method (it can be seen in Fig. 4), we can notice that the Dirlik obtained the most accurate results for α_2 equal to 0.58, 0.78 and 0.94. For irregularity factor equal to 0.28, although the Zhao-Baker presents a closer life than Dirlik when comparing to Rainflow Method, the result generated is non-conservative, what can be seen by the Fig. 4(a) and 4(b). So the Dirlik still shows a better result, whereas $\alpha_{0.75}$ method achieved an over-conservative value for lower irregularity factors and reached closer values for higher irregularity factors. Also the Tovo-Benasciutti method was able to obtain very approximate results even for the lowest α_2 analyzed. In addition, all methods have managed to generate good estimates. Furthermore, when the Al7050-T7451 (k = 5.52 and C = 4.11e+017 MPa^k) is selected as the material for the analysis, it is noticed similar results, however the errors encountered are closer to horizontal black line.

5. CONCLUSION

This research focus on fatigue assessment considering stress histories with irregularity factor varying from 0.30 to 0.94. Analysing the results obtained, it is easy to notice the proximity of frequency domain methods for counting fatigue cycles generated from PDF and the Rainflow Histogram. Moreover, the Dirlik and Zhao-Baker methods obtained quite

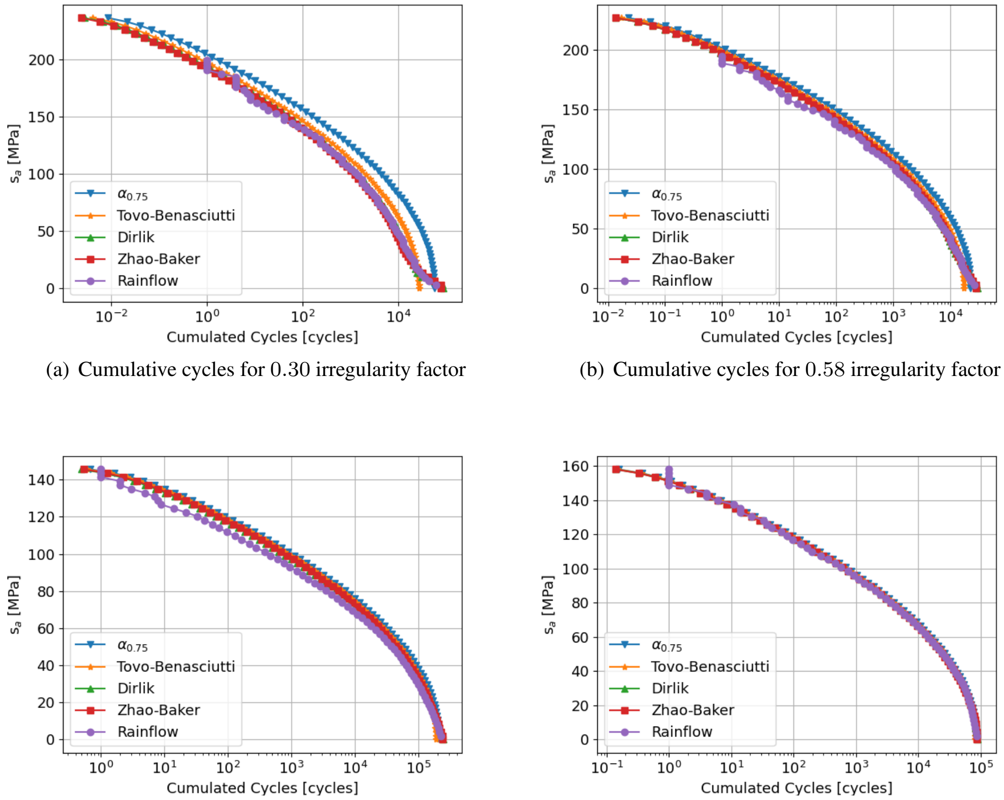

(a) Cumulative cycles for 0.30 irregularity factor
(b) Cumulative cycles for 0.58 irregularity factor
(c) Cumulative cycles for 0.78 irregularity factor
(d) Cumulative cycles for 0.94 irregularity factor

Figure 3. Comparison of Cumulative cycles plots for different irregularity factors.

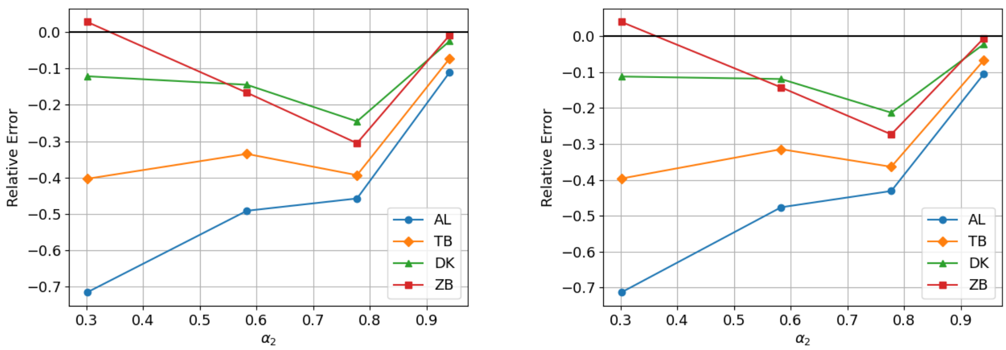

(a) Relative error for 1020 Hot Rolled steel.
(b) Relative error for Al7050-T7451.

Figure 4. Relative error on predicted fatigue life between the frequency domain methods and the rainflow cycle counting method. The loading history of Fig. 1(a) applying the conditions described in Secs. 3.1 and 3.2, along with the material's properties of a 1020 Hot-Rolled steel (a) and Al7050-T7451 (b) were used in the simulation.

approximate results for α_2 equal to 0.58, 0.78 and 0.94, but for α_2 equal to 0.30 the result was non-conservative for Zhao-Baker while Dirlik acchieved a good approximation. Finally, for higher irregularity factors, all methods achieved better agreements. Similar results were noticed for other materials such as the 1020 hot rolled steel and the Aluminum 7050-T7451, although the errors presented by the second one were slightly smaller, when comparing to the absolute value. Thus, it is concluded that the use of methods in the frequency-domain is feasible to obtain a good approximation of the predicted fatigue damage in various materials, since it was possible to obtain close results compared to the Rainflow method with more computational efficiency.

6. REFERENCES

Ariduru, S., 2004. *Fatigue life calculation by rainflow cycle counting method*. Science, The graduate school of natural and applied sciences of middle east technical university, Ankara.

Benasciutti, D., 2005. *Fatigue Analysis of Random Loadings*. Ph.D. thesis, University of Ferrara.

Benasciutti, D., Cristofori, A. and Tovo, R., 2013. "Analogies between spectral methods and multiaxial criteria in fatigue damage evaluation". *Probabilistic Engineering Mechanics*, Vol. 31, pp. 39–45.

Benasciutti, D. and Tovo, R., 2004. "Rainflow cycle distribution and fatigue damage in gaussian random loadings". *Internal Report No. 129, Department of Engineering, University of Ferrara, Italy*.

Benasciutti, D. and Tovo, R., 2005. "Spectral methods for lifetime prediction under wide-band stationary random processes". *International Journal of fatigue*, Vol. 27, No. 8, pp. 867–877.

Bishop, N.W.M. and Sherratt, F., 2000. *Finite Element Based Fatigue Calculations*, Vol. 1. The International Association for the Engineering Analysis Community, Farnham, 1st edition.

Budynas, R.G. and Nisbett, J.K., 2006. *Shigley's Mechanical Engineering Design*. Mc Graw Hill, New York, 8th edition.

Cristofori, A., Benasciutti, D. and Tovo, R., 2011. "A stress invariant based spectral method to estimate fatigue life under multiaxial random loading". *International Journal of Fatigue*, Vol. 33, No. 7, pp. 887–899.

Dirlik, T., 1985. *Application of Computers in Fatigue Analysis*. Ph.D. thesis, The University of Warwick.

Dowling, N.E., 2013. *Mechanical Behavior of Materials*. Pearson, Blacksburg, 4th edition.

eFatigue, 2021. "Material Property Finder". `https://www.efatigue.com/constantamplitude/stresslife/materials/#a`. Accessed 15 may 2021.

Juvinal, R.C. and Marshek, K.M., 2012. *Fundamentals of Machine Components Design*. Wiley and Sons, Michigan, 5th edition.

Lalanne, C., 2003. *Mechanical Vibration and Shock*, Vol. 3. John Wiley and Sons, Hoboken, 3rd edition.

Lalanne, C., 2014. *Fatigue Damage*, Vol. 4. John Wiley and Sons, Hoboken, 3rd edition.

Larsen, C.E. and Irvine, T., 2015. "A review of spectral methods for variable amplitude fatigue prediction and new results". *Procedia Engineering*, Vol. 101, pp. 243–250.

Lutes, L.D., Corazao, M., Hu, S.l.J. and Zimmerman, J., 1984. "Stochastic fatigue damage accumulation". *Journal of Structural Engineering*, Vol. 110, No. 11, pp. 2585–2601.

Mršnik, M., Slavič, J. and Boltežar, M., 2013. "Frequency-domain methods for a vibration-fatigue-life estimation–application to real data". *International journal of fatigue*, Vol. 47, pp. 8–17.

Norton, R.L., 2006. *Machine Design*. Pearson, New Jersey, 3rd edition.

Rice, S.O., 1944. "Mathematical analysis of random noise". *The Bell System Technical Journal*, Vol. 23, No. 3, pp. 282–332.

Tovo, R., 2002. "Cycle distribution and fatigue damage under broad-band random loading". *International journal of fatigue*, Vol. 24, No. 11, pp. 1137–1147.

Weibull, W., 1951. "A statistical distribution function of wide applicability". *Journal of applied mechanics*, Vol. 18, No. 3, pp. 293–297.

Wirsching, P.H. and Light, M.C., 1980. "Fatigue under wide band random loading". *J Struct Div ASCE*, Vol. 106, No. 7, pp. 1593–1607.

Wirsching, P.H. and Shehata, A.M., 1977. "Fatigue under wide band random stresses using the rain-flow method". *Journal of Engineering Materials and Technology*, pp. 205–211.

Zhao, W. and Baker, M.J., 1992. "On the probability density function of rainflow stress range for stationary gaussian processes". *International Journal of Fatigue*, Vol. 14, No. 2, pp. 121–135.